

Rapidity dependence of antiproton to proton ratios in Au+Au collisions at $\sqrt{s_{NN}} = 130$ GeV

I. G. Bearden⁷, D. Beavis¹, C. Besliu¹⁰, Y. Blyakhman⁶, J. Brzychczyk⁴, B. Budick⁶, H. Bøggild⁷, C. Chasman¹, C. H. Christensen⁷, P. Christiansen⁷, J. Cibor³, R. Debbé¹, J. J. Gaardhøje⁷, K. Grotowski⁴, K. Hagel⁸, O. Hansen⁷, A. Holm⁷, A. K. Holme¹², H. Ito¹¹, E. Jakobsen⁷, A. Jipa¹⁰, J. I. Jørdre⁹, F. Jundt², C. E. Jørgensen⁷, T. Keutgen⁸, E. J. Kim⁵, T. Kozik⁴, T. M. Larsen¹², J. H. Lee¹, Y. K. Lee⁵, G. Løvholden¹², Z. Majka⁴, A. Makeev⁸, B. McBreen¹, M. Murray⁸, J. Natowitz⁸, B. S. Nielsen⁷, K. Olchanski¹, J. Olness¹, D. Ouerdane⁷, R. Planeta⁴, F. Rami², D. Röhrich⁹, B. H. Samset¹², S. J. Sanders¹¹, R. A. Sheetz¹, Z. Sosin⁴, P. Staszcz⁷, T. F. Thorsteinsen⁹⁺, T. S. Tveter¹², F. Videbæk¹, R. Wada⁸, A. Wieloch⁴, and I. S. Zgura¹⁰
(BRAHMS Collaboration)

¹ Brookhaven National Laboratory, Upton, New York 11973,

² Institut de Recherches Subatomiques and Université Louis Pasteur, Strasbourg, France,

³ Institute of Nuclear Physics, Krakow, Poland,

⁴ Jagiellonian University, Krakow, Poland,

⁵ Johns Hopkins University, Baltimore, Maryland 21218,

⁶ New York University, New York, New York 10003,

⁷ Niels Bohr Institute, University of Copenhagen, Denmark,

⁸ Texas A&M University, College Station, Texas 77843,

⁹ University of Bergen, Department of Physics, Bergen, Norway,

¹⁰ University of Bucharest, Romania,

¹¹ University of Kansas, Lawrence, Kansas 66045,

¹² University of Oslo, Department of Physics, Oslo, Norway,

⁺ *Deceased*

(April 30, 2001)

Abstract

Measurements, with the BRAHMS detector, of the antiproton to proton ratio at central and forward rapidities are presented for Au+Au reactions at $\sqrt{s_{NN}} = 130$ GeV, and for three different collision centralities. For collisions in the 0 – 40% centrality range we find $N(\bar{p})/N(p) = 0.64 \pm 0.04_{(stat.)} \pm 0.06_{(syst.)}$ at $y \approx 0$, $0.66 \pm 0.03 \pm 0.06$ at $y \approx 0.7$, and $0.41 \pm 0.04 \pm 0.06$ at $y \approx 2$. The ratios are found to be nearly independent of collision centrality and transverse momentum. The measurements demonstrate that the antiproton and proton rapidity densities vary differently with rapidity, and indicate that a net-baryon free midrapidity plateau (Bjorken limit) is not reached at this RHIC energy.

PACS numbers: 25.75.-q

The reaction mechanism between heavy ions at high energies is expected to evolve from

full stopping to complete transparency with increasing collision energy. In the case of full stopping, the baryons of the colliding nuclei will be shifted from the rapidity of the incident beam to midrapidity ($y \approx 0$), leading to the formation of a central zone with significant net-baryon density. In the case of full transparency, also called the Bjorken limit [1], the baryons from the interacting nuclei will, after the collision, also be shifted from beam rapidity, but mid-rapidity will be devoid of original baryons. In this region, the net-baryon density is zero, but the energy density is high. Almost complete stopping is observed for Au+Au reactions at AGS energies ($\sqrt{s_{NN}} \approx 5$ GeV). In reactions between lead nuclei at SPS energies ($\sqrt{s_{NN}} = 17$ GeV), transparency begins to set in, and systematics suggest that maximum baryon density occurs at energies intermediate between AGS and SPS (see e.g. [2,3]). The situations of maximum baryon density and of vanishing net-baryon density at midrapidity give rise to entirely different initial conditions for the possible creation of a deconfined quark-gluon system.

The rapidity dependence of the antiproton to proton ratio in collisions between Au nuclei at the Relativistic Heavy Ion Collider (RHIC), Brookhaven National Laboratory, is investigated for $\sqrt{s_{NN}} = 130$ GeV, the highest center of mass energy yet achieved in collisions between heavy nuclei in the laboratory. The data were collected with the BRAHMS detector during the final 2 weeks of the first RHIC run in August and September 2000, where the beam luminosity reached $\approx 10\%$ of the nominal design value ($2 \times 10^{26} \text{cm}^{-2} \text{s}^{-1}$). We present measurements of the $N(\bar{p})/N(p)$ rapidities $y \approx 0, 0.7$ and 2 as a function of collision centrality and transverse momentum together with $N(\pi^-)/N(\pi^+)$ ratios at $y \approx 0, 1$ and 3 . The beam rapidity is 4.95 . The measurements provide the first particle ratios over an extended rapidity range at RHIC energies. We find that while the pion ratios are close to unity, the measured antiproton to proton ratio decreases from $0.64 \pm 0.04_{(stat.)} \pm 0.06_{(syst.)}$ at $y \approx 0$ and $0.66 \pm 0.03_{(stat.)} \pm 0.06_{(syst.)}$ at $y \approx 0.7$ to $0.41 \pm 0.04_{(stat.)} \pm 0.06_{(syst.)}$ at $y \approx 2$ for 0-40% collision centrality. The results show that a net-baryon free midrapidity region has not been attained, although the $N(\bar{p})/N(p)$ ratio is the highest that has been measured so far in nucleus-nucleus collisions. Recently, the STAR collaboration has measured similar particle ratios at $y \approx 0$ in a narrower momentum range [4] and their results agree well with the $y \approx 0$ measurements presented here.

The BRAHMS detector system [5] used in the present measurements consists of two independent magnetic spectrometers that can be positioned over an angular range from 2.3° to 30° (forward spectrometer, FS) and from 25° to 90° (midrapidity spectrometer, MRS) with respect to the beam line. A scintillator tile multiplicity array (TMA) measures charged particle emission in the central pseudorapidity region ($-2.0 < \eta < +2.0$) and is used for off-line centrality selection. This detector consists of 38 square tiles of plastic scintillators ($12 \times 12 \times 0.5 \text{ cm}^3$). The tiles are grouped in rows of 8 to form a tube of hexagonal cross section with the axis along the beam pipe, such that no tile is placed in the MRS and FS acceptances. Two global detector systems cover forward angles. The Zero Degree Calorimeters (ZDC) at ± 18 m measure spectator neutrons [6]. The Beam-Beam Counters (BB) consist of two arrays with a total of 70 phototubes, each with a Cerenkov radiator, positioned ± 2.15 m and measure charged hadrons in the pseudo-rapidity range of $3.0 < |\eta| < 3.8$. These two systems are used to define collision events by two simultaneous measurements of the interaction vertex position.

For each actual vertex position the total energy deposited in each ring of TMA tiles

is determined. This energy loss signal is transformed to a charged particle multiplicity via division with the expected average energy deposited by one primary charged particle in a tile at its corresponding pseudo-rapidity. Centrality cuts are applied by selecting appropriate ranges in the multiplicity spectrum. The cuts can be expressed in terms of the fraction of the nuclear reaction cross section by normalization to the integral of the TMA spectrum obtained with a minimum bias trigger. This trigger requires energy deposition in each of the two ZDCs above 25 GeV with the additional condition of at least one tile having a hit. Comparing to simulations with the HIJING code this requirement selects events corresponding to $\approx 99 \pm 2\%$ of the nuclear interaction cross section. Centrality bins from 0 to 10 %, 10 to 20 %, and 20 to 40 %, of this event selection were used in the analysis.

In the present measurements the MRS was operated at both 90° and 40° and the FS at 4° . The magnets of the two spectrometers were operated at fields allowing the reconstruction of particle tracks with momenta above ≈ 0.2 GeV/ c in the MRS and above ≈ 2 GeV/ c in the FS. The solid angles subtended by the MRS and FS are 6.5 msr and 0.8 msr, respectively. Each spectrometer consists of two Time Projection Chambers (TPCs) positioned on either side of a dipole magnet and followed by a segmented scintillator time of flight (TOF) wall for particle identification (PID). In the case of the FS this tracking and PID arrangement is preceded by an additional dipole magnet to sweep particles away from the beam and reduce background.

Particle momenta are determined by projecting the straight line tracks as reconstructed in the two TPCs to the magnet and calculating the bending angle of matched tracks using an effective edge approximation. The momentum resolution is $\delta p/p \approx 0.01 \cdot p$ for the FS, and for the MRS $\approx 0.04 \cdot p$ (90°), and $\approx 0.03 \cdot p$ (40°) at the field settings used. MRS tracks are required to originate from the primary vertex as determined by the BB counters within ± 5 cm horizontally, and ± 5 cm vertically from the nominal beam position. Tracks in the FS have the same vertical, but a much looser horizontal matching requirement (± 12 cm) due to the uncertainty associated with projecting tracks back to the beam line. PID requires not only a TOF measurement, but also the determination of the flight distance and thus of the collision vertex position on an event by event basis. The BB counters have an intrinsic time resolution of 65 ps and permit a determination of the collision vertex position to a precision of ≈ 2 cm by measuring the difference in arrival time of particles in the two arrays, assuming that particles travel with the velocity of light. This method is confirmed by determining the vertex by projecting tracks determined in the first TPC of the MRS back to the beam plane. The collision vertex distribution was approximately of Gaussian shape with $\sigma \approx 70$ cm. We select events with vertex between ± 15 cm for MRS and ± 40 cm for FS, respectively. The two TOF arrays are positioned at 4.3 m (MRS) and 8.6 m (FS) from the nominal interaction vertex position, respectively. The overall time resolution was determined to be $\sigma(\text{TOF}) \approx 120$ ps.

Kaons and protons are separated in the momentum range $p < 2.4$ GeV/ c and $p < 4.5$ GeV/ c in the MRS and FS, respectively. Kaons and pions can be separated up to $p = 1.6$ GeV/ c in MRS. In the FS, kaons could not be cleanly separated from pions, although the $N(\pi^-)/N(\pi^+)$ ratio for $0.15 < p_t < 0.3$ GeV/ c was determined with only a small kaon contamination. Figure 1 demonstrates the PID achieved in the MRS and FS. The lower two panels show the m^2 spectra obtained for positively charged particles (π^+, K^+, p) and the upper two panels for negative particles (π^-, K^-, \bar{p}). These distributions were calculated

using $m^2 = p^2(t^2/L^2 - 1)$, where p , t , and L denote the particle momentum, TOF, and flight distance, respectively. The MRS data shown are from $0.4 < p_t < 2.4$ GeV/ c , while the FS data are from $0.15 < p_t < 0.55$ GeV/ c .

The particle yield in the FS is determined by selecting tracks having a TOF within a $\pm 2\sigma$ band of the expected TOF vs. momentum for a given particle type. The results of such cuts for pions and protons are shown in Fig. 1. There is a systematic uncertainty that causes a small shift in the m^2 scale vs momentum. The effect on extracted particle ratios from the prescribed method is estimated to be small. In the MRS, where the momenta are much lower and the particle peaks better separated, the yields can be determined by applying cuts in the m^2 spectra, as seen in Fig. 1. The number of particles measured at either polarity is normalized to the number of collision events defined by the BB-ZDC coincidences fulfilling a given centrality cut described above and the ratios are calculated.

The acceptances for the spectrometers for positively charged particles at one field are equal to the acceptances for negatively charge particles at the opposite polarity. Thus in ratios of numbers of particles, measured at opposite field polarities most systematic errors cancel out. The ratios have been corrected for losses of antiprotons due to annihilation evaluated by GEANT simulations to be less than 2 % in the MRS and about 3.5 % in the FS. It is noted that background from misidentified tracks and from the tails of kaon and pion peaks are negligible for the measurements at 90° and 40° . At forward angles the contributions from background tracks increase but are still small, and affect the extracted ratios negligibly ($< 1\%$). In the MRS, the background contribution from slow protons, arising mainly from the interaction of pions with the Be beam pipe, is $\approx 10\%$ for the lowest p_t bin. The data have been corrected for this effect. In the FS this contribution is found to be negligible. The main sources of systematic uncertainties in the particle ratios are due to normalizations, corrections for the background of slow protons, and from corrections for antiproton absorption. The normalizations contribute less than $\pm 5\%$.

Figure 2 shows the dependence of the measured $N(\bar{p})/N(p)$ ratios on collision centrality and on particle transverse momentum. Ratios were corrected for antiproton absorption as described above. Figure 2(a) shows the centrality dependence for data summed over all momentum bins, while Fig. 2b shows the p_t dependence for data summed over all centrality bins. The vertical error bars represent statistical errors only. It is seen that the centrality dependence of the ratio is small for the three considered rapidities. The $N(\pi^-)/N(\pi^+)$ ratios (not shown) exhibit a similar lack of centrality and p_t dependence.

The ratios shown in Fig. 2 have not been corrected for protons and antiprotons that originate from weak decays of hyperons (Λ , Σ , *etc*). The correction factors will in general depend on the relative production ratios of hyperons ($N(H)$) and primary baryons ($N(B)$) and their antiparticles, and on the relative slopes of their spectra. We have studied the magnitude of the corrections using various assumptions as input to GEANT simulations. Assuming primary $N(H)/N(B)$ ratios of up to 0.5 we find that the correction to the quoted ratios is less than $\pm 5\%$ for $N(\bar{H})/N(H)$ between 0.4 and 0.8 ($y \approx 0$) and between 0.3 and 0.5 ($y \approx 2$).

Figure 3 summarizes the rapidity dependence of the measured particle ratios calculated for the 0 – 40% most central collisions. The upper and lower panel depict the $N(\pi^-)/N(\pi^+)$ and $N(\bar{p})/N(p)$ ratios, respectively. It is seen that, while the pion ratio is independent of rapidity and consistent with unity, the antiproton to proton ratio drops significantly with

increasing rapidity.

The $N(\bar{p})/N(p)$ ratio of 0.64 found here at $y \approx 0$ is considerably higher than the similar ratios measured in Pb+Pb collisions at the SPS ($\approx 0.07 - 0.15$ at $\sqrt{s_{NN}} = 17$ GeV) [7,8] and at the AGS ($\approx 2.5 \cdot 10^{-4}$ at $\sqrt{s_{NN}} = 5$ GeV) [9]. It is, in fact, close to the p+p result (0.61 ± 0.10) from the ISR [10] at $\sqrt{s_{NN}} = 63$ GeV and $p_t \approx 0.3 \text{ GeV}/c$, and below the value obtained by extrapolating the p+p systematics to 130 GeV CM energy. The rapidity dependence of the ratios is of particular interest. The $N(\bar{p})/N(p)$ at $y \approx 0$ and ≈ 0.7 are approximately the same, consistent with the formation of a plateau around mid-rapidity. The decrease in the ratio over the next unit of rapidity is larger than observed in A+A collisions at lower energies, but are very similar to the p+p result at roughly half the CM energy [11].

Finally, in Fig. 3, we compare the measured ratios to calculations using the HIJING model [12], the FRITIOF 7.02 string model [13] and the UrQMD cascade model [14] using the same centrality cuts as in the data analysis. Hyperon decays have not been included in the calculations shown, but affect the results by less than 5 %. All three models reproduce the observed pion ratios well. FRITIOF reproduces our $N(\bar{p})/N(p)$ ratios, while overpredicting (by ≈ 30 %) the charged particle yield at $\eta \approx 0$ [15]. This is due to a significant degree of stopping in the model. On the other hand, HIJING which describes the overall charged particle yields at $\eta \approx 0$ fails in describing the antiproton to proton ratio. This feature of the model is related to the small stopping of the projectile baryons. The UrQMD model, which is not a partonic model, under predicts the ratio by nearly a factor of two. These models exemplify the present theoretical understanding of heavy ion collisions in this new energy regime. None of the models offer a consistent description of the observed features.

In summary, the BRAHMS experiment has measured the ratio of positive and negative pions and protons at central and forward rapidities. We find that the pion ratios are close to unity as would be expected at these energies, where about 4000 charged particles (predominantly pions) are produced per central collision. We find, however, that for central collisions at $\sqrt{s_{NN}} = 130$ GeV the ratio of antiprotons to protons is still significantly below unity at midrapidity and decreases towards forward rapidity. The rapidity dependence serves as an indicator of the balance between baryon number transport to the central region and antibaryon and baryon pair production. This suggests that there is still a significant contribution from participant baryons over the entire rapidity range and that the full transparency of the Bjorken model has not been reached. Nevertheless, reactions at the present energy evidence the highest antiparticle/particle ratios so far observed in energetic nucleus-nucleus collisions.

The BRAHMS collaboration wishes to thank the RHIC team for the great efforts that have led to the successful startup of the collider and for the support to the experiment. This work was supported by the Division of Nuclear Physics of the Office of Science of the U.S. Department of Energy under contracts DE-AC02-98-CH10886, DE-FG03-93-ER40773, DE-FG03-96-ER40981, and DE-FG02-99-ER41121, the Danish Natural Science Research Council, the Research Council of Norway, the Jagiellonian University Grant, the Korea Research Foundation Grant, and the Romanian Ministry of Education and Research (5003/1999,6077/2000).

REFERENCES

- [1] J. D. Bjorken, Phys. Rev. **D27**, 140 (1983).
- [2] N. Herrmann, J. P. Wessels and T. Wienold, Ann. Rev. Nucl. Part. Sci. **49**, 581 (1999).
- [3] F. Videbæk and O. Hansen, Phys. Rev. **C52**, 2584 (1995).
- [4] C. Adler et al., The STAR collaboration, Phys. Rev. Lett. (in print).
- [5] D. Beavis et al., ‘Conceptual Design Report for BRAHMS’, BNL-62018; I.G. Bearden et al., The BRAHMS collaboration, Nucl. Instr.& Methods, (in preparation).
- [6] C. Adler et al., Nucl. Instr. & Methods,(2001) (in print), ([/xxx.lanl.gov/nuclex/0008005](http://xxx.lanl.gov/nuclex/0008005)).
- [7] I. G. Bearden et al., NA44 collaboration, J. Phys. G, Nucl. Part. **23**, 1865 (1997); M. Kaneta Ph. D. Thesis, 1998, University of Hiroshima.
- [8] F. Sickler et al., The NA49 collaboration; Nucl. Phys. **A661**, 45c (1999); G. E. Cooper, Ph. D. Thesis, 2000, University of California, Berkely.
- [9] L. Ahle et al., The E802 collaboration, Phys. Rev. Lett. **81**, 2650 (1998).
- [10] K. Guettler et al., Nucl.Phys. **B116**, 77 (1976).
- [11] P. Capiluppi et al., Nucl. Phys. **B79**, 189 (1974).
- [12] HIJING 1.36 with Parton shadowing and Jet quenching. X-N. Wang and M. Gyulassy, Phys. Rev. **D44**, 3501 (1991).
- [13] B. Anderson et al., Z. Phys. **C57**, 485 (1993); H. Pi, Comp. Phys. Comm. **71**, (1992).
- [14] S. A. Bass et al., Prog. Part. Nucl. Phys. **41** 225 (1998); M. Bleicher et al. J. Phys. G. Nucl. Part **25**, 1859 (1999).
- [15] B. Back et al., Phys. Rev. Lett. **85**, 3100 (2000).

FIGURES

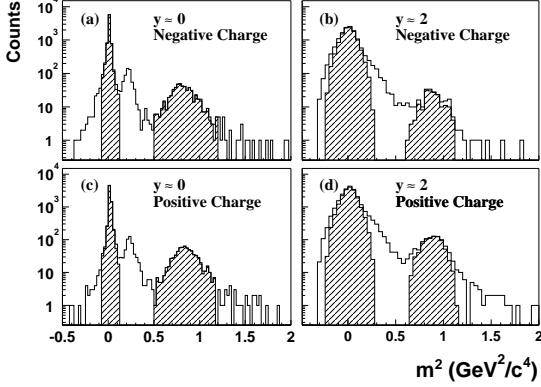


FIG. 1. Distributions of m^2 for charged particles identified in the BRAHMS spectrometers. Left panels (a) and (c) show data from 90° for negatively and positively charged particles, respectively. The hatched areas show the pions selected for analysis in the momentum range $p < 1.6$ GeV/ c and $-0.075 < m^2 < 0.125$ and the protons for $p < 2.4$ GeV/ c and $0.5 < m^2 < 1.2$. The right panels (b) and (d) show data from 4° . The hatched region for these panels shows yield of particles selected for analysis on the basis of fiducial cuts on time-of-flight for a momentum range of $2 < p < 4$ GeV/ c .

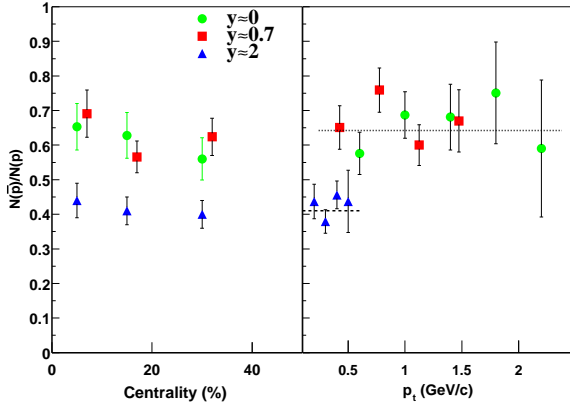


FIG. 2. The left panel shows the centrality dependence of the $N(\bar{p})/N(p)$ ratios for the three rapidity values: $y \approx 0$ (filled circles), $y \approx 0.7$ (open squares) and $y \approx 2$ (filled triangles). Only statistical errors are shown. The data points for $y \approx 0.7$ are shifted slightly for display purpose. The centrality percentages are described in the text. The right panel shows the transverse momentum dependence of the measured $N(\bar{p})/N(p)$ ratio for the same three rapidity intervals for events selected from the 0 – 40% centrality cut. The upper dotted line shows the average ratio for $y \approx 0$, while the dashed line for $y \approx 2$.

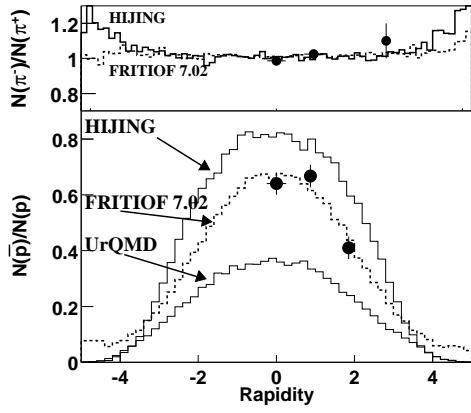


FIG. 3. Comparison of the measured $N(\bar{p})/N(p)$ (lower panel) and $N(\pi^-)/N(\pi^+)$ (upper panel) ratios to model predictions. The data shown are for 0 – 40% central events and integrated over the transverse momentum range shown in Fig. 2. The three model calculations (HLJING, FRITIOF, and UrQMD) are shown for comparison. See text for details.